

Methanol Adsorption in Zeolites—A First-Principles Study

Rajiv Shah,^{*,†} Julian D. Gale,[‡] and Michael C. Payne[†]

Cavendish Laboratory (TCM), University of Cambridge, Madingley Road, Cambridge CB3 0HE, U.K., and Department of Chemistry, Imperial College, South Kensington SW7 2AY, U.K.

Received: February 7, 1996; In Final Form: April 24, 1996[⊗]

The methanol to gasoline (MTG) conversion process, using a zeolite catalyst, is of major commercial importance. However, the first step of the reaction, involving methanol adsorption on the zeolite catalyst, is still not well understood. This paper describes first-principles calculations performed on periodic zeolite models to investigate the nature of methanol adsorption. We have examined a number of possible geometries for this adsorption and found that the nature of the adsorbed species can depend on the particular zeolite structure. In more open ring structures, as found in chabazite, the stable form of methanol is found to be protonated, in contrast to results of previous calculations on cluster models. However, in the sodalite structure methanol is found to be simply physisorbed. The vibrational spectra of the adsorbed species have been studied and compared to experimental results. It is found that both chemisorbed methanol and physisorbed methanol give strongly red-shifted O–H stretching frequencies, but the former can be distinguished by the H–O–H bending mode.

1. Introduction

Zeolites are microporous aluminosilicate structures with many applications as acid catalysts.¹ One important example is the methanol to gasoline (MTG) process,² which has accounted for up to 30% of New Zealand's gasoline supply. This process has been the subject of numerous experimental and theoretical studies, but it is still not particularly well understood. Even the first stage of the reaction, the adsorption of methanol at a Brønsted acid site in the catalyst, has been the subject of much debate. Experimental results from IR spectroscopy^{3,4} and NMR work^{5,6} were interpreted as showing transfer of the acidic proton from the zeolite to the adsorbate, or chemisorption, in keeping with the notion of zeolites as strong acid catalysts. Subsequent theoretical work made the interpretation of these results a matter for debate. Initial work by Sauer *et al.*⁷ suggested that this picture was correct, but this was later shown to be an artifact due to the use of symmetry constraints.⁸ More recent cluster results using both gradient-corrected density functional theory⁸ and analysis at the MP2 level⁹ agree that proton transfer from the framework to the adsorbate is unstable, with the protonated intermediate being a transition state for hydrogen exchange between the different zeolite lattice oxygens adjacent to aluminum. Thus, the stable adsorption geometry is predicted to be simple physisorption of methanol, forming two hydrogen bonds to form a six-membered ring with the acid site. Further work^{10,11} has considered how methanol may be activated without proton transfer and examined possible reactive intermediates such as the formation of surface methoxy groups as the next stage of the reaction.

A major uncertainty of these theoretical models has been their reliance on the cluster approximation, namely, that a zeolite may be modeled by treating only a few atoms of the structure without needing to consider the effects of the rest of the framework. In the cluster, dangling bonds of the cluster are saturated with hydrogen atoms, which have been shown to affect the acidity of the cluster.¹² Different zeolite structures are observed to have varying levels of catalytic activity, so that

framework topology should be expected to have an important effect. Most notably, the cluster approach ignores the long-range electrostatic potential, which may have a considerable effect given the partially ionic nature of zeolites. Some attempts have been made to remedy this by embedding such clusters in a set of point charges chosen to reproduce the bulk potential^{13,14} and even in the full wave function of the perfect crystal.¹⁵ However, such models still suffer from uncertainty over boundary effects, etc. Small clusters will also neglect the interaction of an adsorbed molecule with the rest of the cage or channel in which it is adsorbed, and a single cluster does not allow proper consideration of all possible adsorption geometries, so that different clusters must be used that do not allow consistent cancellation of errors. Relaxation effects are another shortcoming of the cluster model—it is difficult to correctly simulate the forms of relaxation possible in the bulk, and the imposition of symmetry constraints can lead to problems, as discussed earlier. Two extremes can be used: allowing the cluster to be completely unconstrained, which overestimates the freedom of relaxation, or fixing boundary atoms, which in small clusters will only allow limited optimization.

To avoid these uncertainties, we have adopted a different approach: use of periodic boundary conditions to simulate the full zeolite structure. Such an approach has been used in Hartree–Fock calculations of ammonia adsorption in zeolites by Teunissen *et al.*¹⁶ and local density functional calculations of zeolitic acid sites.¹⁷ Most commercially used zeolite structures have too large a unit cell for this to be feasible with existing computer resources. For instance, the unit cell of ZSM-5, the commercial catalyst used for the MTG process, has 288 atoms. Hence, we have concentrated our initial studies on the chabazite structure,¹⁸ which, having only 36 atoms in the unit cell, reduces the problem to a manageable size. As chabazite has been observed to be an active catalyst for the condensation of methanol to dimethyl ether,¹⁹ this constitutes a realistic model. The structure has 3D channels with eight-ring windows. This system has been studied using first-principles density functional theory methods, which are described in the next section. As a first step we have considered the case of only one Brønsted acid site per unit cell, and the results for this are described in section 3. A variety of possible geometries for

[†] University of Cambridge.

[‡] Imperial College.

[⊗] Abstract published in *Advance ACS Abstracts*, June 15, 1996.

methanol adsorption at a single chabazite acid site are considered in section 4, and the characteristics of the most stable adsorbed form are considered in section 5, including the nature of bonding and the IR frequencies. To examine the potential effect of structure on catalytic activity, we have made a comparison with methanol adsorption in sodalite, as described in section 6, and by comparing the IR frequencies for this system, we offer an interpretation of the experimentally observed spectra.

2. First-Principles Calculations

Recent improvements in parallel computing, coupled with improved algorithms,²⁰ have now made it feasible to study zeolitic problems by using first-principles methods within the framework of density functional theory.^{21,22} Therefore, we have chosen to utilize such techniques for the present study. Because of the importance of obtaining a reliable description of the intermolecular forces, it is necessary to go beyond the local density approximation. Therefore, the exchange-correlation energy is calculated by using the generalized gradient approximation (GGA) of Perdew and Wang,²³ represented on a normal density grid.²⁴ This allows GGA calculations to be performed with approximately the same memory and time requirements as LDA calculations.

As mentioned earlier, our calculations are carried out using periodic boundary conditions. This allows the use of a plane-wave basis set, which has a number of advantages, including the ability to systematically take the basis set to convergence and straightforward calculation of the forces on the ions. Furthermore, as the basis set is not atom centered, there is no basis set superposition error (BSSE), which improves the accuracy of the forces relative to a comparable molecular calculation. The nuclei and core electrons are represented by norm-conserving pseudopotentials.²⁵ The potentials for carbon and oxygen have been optimized by using kinetic energy filter tuning^{26,27} to reduce the size of the plane-wave basis set required. By monitoring the convergence of calculated properties of bulk quartz and a methanol molecule a plane-wave cutoff of 650 eV was found to be sufficient. The pseudopotentials used were nonlocal, with the projection onto the wave functions being carried out in real space²⁸ to reduce the cost of this operation from $O(N^3)$ to $O(N^2)$. To further reduce the computational cost, the potentials for carbon and oxygen were projector reduced,²⁹ so that only the s nonlocal component in the potential was retained. All of the pseudopotentials used were tested extensively to ensure their accuracy. For hydrogen a bare Coulomb potential was used, as previous experience has shown that, at this level of plane-wave cutoff, the convergence of energy differences is controlled by the oxygen pseudopotential.³⁰ Brillouin zone sampling was performed only at the Γ point. Tests of increasing plane-wave cutoff and Brillouin zone sampling showed that the values used were sufficient to converge energy differences for this system to within 2 kJ mol⁻¹.

One remaining possible source of error in these calculations could be the use of the GGA functional. Although difficult to estimate, this was tested by a careful calculation of the gas phase proton affinity of methanol. As the question of proton transfer to methanol from the zeolite is vital in this work, this forms a sensitive test of the accuracy of our method. Calculations of a methanol molecule, CH₃OH, and of the methoxonium ion, (CH₃OH₂)⁺, were carried out in cubic cells of increasing size. The energy of a methanol molecule was found to converge to within 1 kJ mol⁻¹ for a 9 Å cell. In the case of the charged molecule, special problems are associated with the use of periodic boundary conditions. A neutralizing background must be introduced to avoid divergence of the electrostatic energy,

TABLE 1: Energies and IR Frequencies of Different Acid Sites in Chabazite^a

acid site	energy (eV)	ν_{OH} (cm ⁻¹)
O1	0.00	3875
O2	0.07	3920
O3	0.04	3820
O4	0.09	3815

^a The zero of energy is taken to be O1, the most stable site. The frequencies are as calculated in the harmonic approximation. Estimates of the anharmonic effect suggest that these may be reduced by about 200 cm⁻¹.

which introduces spurious terms of $O(L^{-1})$ (due to the interaction of the periodic array of charges with the neutralizing background) and $O(L^{-3})$ (due to the interaction of the background with the average potential of the system). These can be corrected for analytically by using the formulae given by Leslie and Gillan³¹ and by Makov and Payne,³² speeding the convergence with respect to cell size to be similar to the methanol molecule. In this way the proton affinity is calculated to be -774 kJ mol⁻¹, which is in good agreement with the experimental value³³ of -778 kJ mol⁻¹.

The forces on the ions were obtained by using the Hellman–Feynman theorem, and these were used to relax the ions to equilibrium by using a BFGS technique.³⁴ The relaxation was continued until the forces on all of the ions were less than 0.03 eV Å⁻¹. All of the ions were allowed to relax at constant volume, the initial cell size being fixed at that obtained by a shell-model optimization for the purely siliceous material. For the trigonal rhombohedral unit cell, this gave a cell length of 9.186 Å and an angle of 94.76°. It should be noted that the ionic relaxation procedure adopted will always take the ions to a lower energy configuration with each step. Generally, it will take the structure to the nearest local minimum. Although in principle the relaxation might stop at a saddle point, in practice numerical noise in the forces will prevent this.

The calculations were carried out on a parallel computer by using the CETEP code.³⁵ By using a Cray T3D, a single-point energy calculation took about 15 node hours, and it was generally found that about 50 steps are needed to converge the geometry to the required accuracy. We should stress that the method is fully *ab initio* and that all of the atoms were allowed to relax freely, without the application of any constraints other than the periodic boundary conditions imposed on the supercell, the size and shape of which are kept fixed.

3. Brønsted Acid Sites

As a first step in this investigation, we have examined isolated Brønsted acid sites in chabazite.³⁶ These are formed by substituting a silicon atom by an aluminum atom, with an associated proton that maintains charge neutrality. Although from the experimental Si:Al ratio of 3 one would expect three out of the twelve T sites in the unit cell to be substituted by aluminum, we have initially restricted our study to a form with only one Al site per unit cell to reduce the number of permutations to be considered. In fact, a high-silica form of chabazite, SSZ-13, has recently been prepared,³⁷ which would closely correspond to our model system.

The chabazite structure contains a single unique tetrahedral site in the asymmetric unit, leading to four possible acid site configurations, depending on which oxygen the proton is coordinated with. The relative energies are tabulated in Table 1, along with O–H stretching frequencies as calculated in the harmonic approximation. The values differ slightly from those in ref 36 due to the use of more accurately relaxed atomic structures here. Although O1 is the most stable site, at typical

TABLE 2: Selected Angles and Distances for the Illustrated Adsorption Geometries Found Compared to Isolated Methanol and Chabazite Acid Site (Column A) and Isolated Methoxonium (Column B)

	A	B	Figure 4	Figure 6	Figure 8	Figure 9	Figure 12	Figure 13
O1-H1 (Å)	0.98	0.98	1.04	1.30	1.28	0.98	1.57	1.45
O1-H2 (Å)		0.98	1.06	0.97	0.97 ^c	0.97	0.98	0.98
H1-O1-H2 (deg)		109	95	100	108 ^d	112 ^e	95	106
O3-H1 (Å)	0.97		1.54	1.15	1.17	1.91	1.03	1.06
O2-H2 (Å)			1.43	2.02	2.45	1.94	1.91	1.76
C-O1 (Å)	1.45	1.52	1.45	1.46	1.47	1.51	1.45	1.44
Al-O2 (Å)	1.66		1.71	1.61 ^a	1.66	1.67	1.69	1.64 ^f
Al-O3 (Å)	1.80		1.70	1.62 ^b	1.75	1.67	1.82	1.79

^a Si-O2. ^b Si-O3. ^c O1-H3. ^d H1-O1-H3. ^e H3-O1-H4. ^f Si-O2.

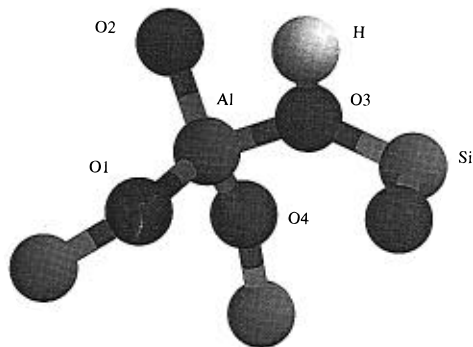


Figure 1. Local geometry of the Brønsted acid site in chabazite, in this case for proton bound to O3. The O3-H distance is 0.97 Å, Al-O3 is 1.85 Å, other Al-O is 1.65 Å, and O3-Si is 1.69 Å. The Al-O-Si angle is 136°, and the O-H bond lies 6.8° out of the Al-O-Si plane.

operating temperatures of around 700 K, O3 is less than kT higher in energy. It is possible also that the protons may redistribute in the presence of an adsorbate. The frequencies were obtained by a quadratic fit to the energy calculated for various displacements of H along the O-H direction, with the motion of the framework oxygen accounted for to the first order by use of the reduced mass of the OH pair in the calculation. The frequencies obtained are slightly higher than typical experimental values, but this is prior to the application of corrections for anharmonic effects. These may be estimated by obtaining a cubic fit to the energy vs distance plot and treating this as a low-order expansion of a Morse potential (see Appendix). From this method we estimate that the anharmonic effect will reduce the calculated frequencies by about 200 cm^{-1} , bringing them into good agreement with typical zeolite hydroxyl stretching frequencies. This is similar to the estimate by Sauer *et al.*³⁸ of 150 cm^{-1} for the anharmonic effect.

An examination of the charge density and geometry compared to purely siliceous chabazite shows similar features for all four sites. There is a depletion of charge between aluminum and the neighboring oxygens and a lengthening of the bonds, in particular that between Al and the protonated oxygen,³⁶ the latter being about 1.8 Å and the other Al-O bonds being about 1.65 Å. It is notable that these bond lengths are about 0.1 Å shorter than those found in cluster studies.³⁹ This could be partly attributed to the fact that in our simulation the unit cell volume is kept fixed. However, the framework connectivity will also restrict the degree of relaxation possible to accommodate Al in the structure. As a result of the increased strain on the Al-O[H] bond, the acidity may be increased relative to cluster models. The local geometry is illustrated in Figure 1. Looking at the total charge density (Figure 2) shows that the proton lies in the charge cloud of a framework oxygen and that most of the charge is concentrated on the framework oxygen. In the siliceous region of the framework, our total charge density resembles that obtained by Aprà *et al.*⁴⁰ We have examined

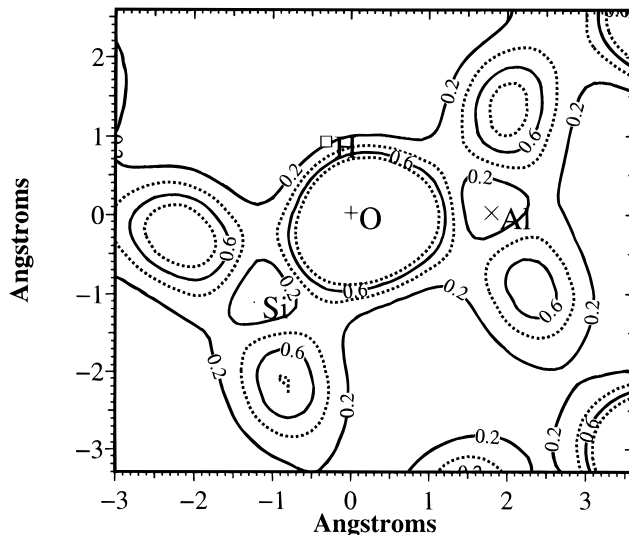


Figure 2. Valence charge density of chabazite around an isolated Brønsted acid site. The plot is taken in the Al-O-Si plane, and the contours are in units of $e \text{ \AA}^{-3}$.

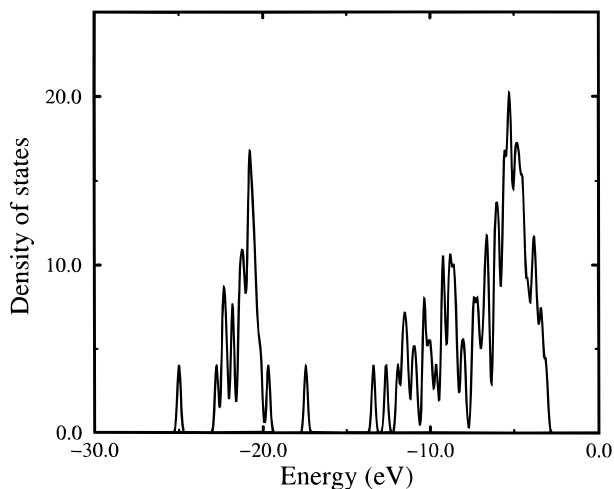


Figure 3. Electronic density of states for the Brønsted acid site in chabazite. The density of states is in eV^{-1} , smeared by a Gaussian of width 0.1 eV.

the contribution to the charge density from each of the electronic bands to build up a picture of this bonding. The electronic density of states is shown in Figure 3. The lowest lying state, at -25 eV, is found to resemble a σ bond between an oxygen p orbital and the hydrogen 1s. The next group of 24 bands (one per oxygen) resembles oxygen s orbitals, with the highest one, slightly separated off at -17.4 eV, showing some mixing with the hydrogen 1s orbital. The following 24 states, from -13.4 to -7.4 eV, consist of oxygen p orbitals directed approximately along the Si-O and Al-O bonds. The remaining 47 states are oxygen p orbitals transverse to the bonds (two for

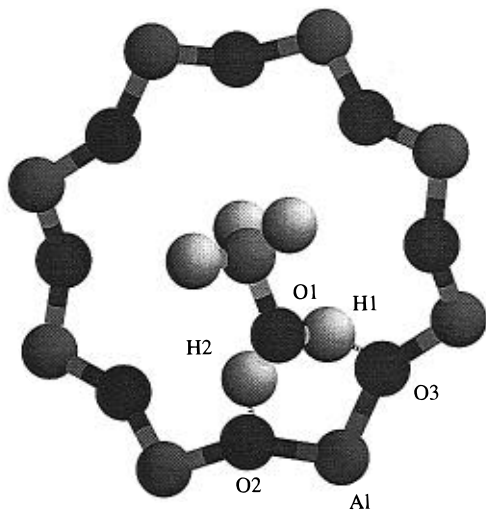


Figure 4. Equilibrium geometry found for six-membered-ring geometry, bridging across an Al site. Distances and angles are given in Table 2.

each oxygen, less one that formed the O—H bond in the lowest lying orbital). The fact that the latter two sets of bands are not well separated in energy suggests that the bonding may be seen as largely ionic, although since there is no overlap in energy ranges this suggests some covalent interaction of p orbitals lying along the bonds with the Si orbitals. The interaction of the acidic proton with the framework is, however, clearly covalent.

4. Methanol Adsorption Geometries

In principle there are a large number of ways in which methanol may bind to a zeolite catalyst. Although it is known from spectroscopic evidence that methanol is initially adsorbed at Brønsted acid sites,³ this still leaves a range of possibilities. We have considered a number of these, which we discuss in the following.

4.1. Six-Membered Ring, Bridging across Al. Previous cluster-based work^{8,9} has suggested the formation of a six-ring arrangement of the methanol OH group and a zeolitic O—Al—O[H] group. This has also been proposed to explain the results of *in situ* spectroscopic work in this area.^{3,4} As discussed in section 1, much debate has centered on the question of whether the proton can be transferred from the framework to the methanol to form a stable chemisorbed species or whether the methanol is simply physisorbed.

In the case of chabazite, the one unique tetrahedral unit has six edges that methanol could bridge across in this way. We have chosen to study the case of bridging between O2 and O3, which has minimal steric hindrance of the molecule compared to some other possible configurations. In this way, methanol lies in the eight-ring window of the chabazite structure. Three starting geometries were tried: with the proton coordinated to O2, coordinated to O3, and transferred to the methanol. In all three cases, when the structure was allowed to relax to the closest local energy minimum, the same geometry was found, that of the chemisorbed form. It has proved impossible to locate a minimum corresponding to methanol simply being physisorbed, and so we conclude that for this geometry the protonated form of adsorbed methanol is the most stable, with no barrier to proton transfer. Thus, our results are, even on a qualitative level, quite different from previous work. Possible reasons for this are discussed in section 6.

The geometry of the stable complex found is illustrated in Figure 4. The hydrogen-bonded distances are as small as 1.43 Å. These are very short, which is consistent with the observed

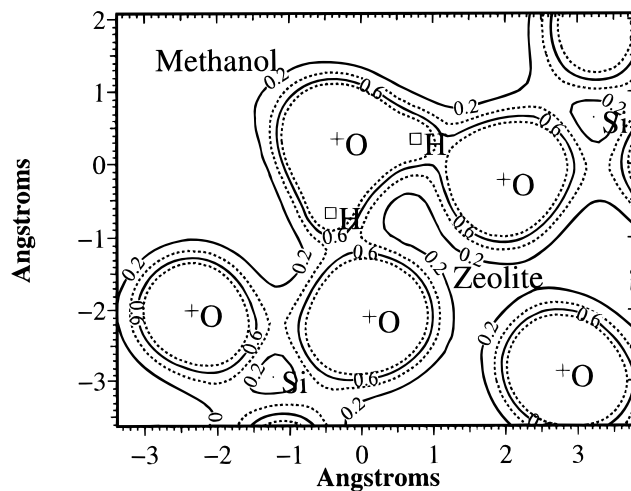


Figure 5. Valence charge density for methanol adsorbed as shown in Figure 4. Contours are in $e \text{ \AA}^{-3}$.

trend of decreasing O...H distances with increasing cluster size in such calculations.⁴¹ The valence charge density is shown in Figure 5, clearly demonstrating that the proton is no longer bound to the zeolite, but to the methanol. However, very strong polarization of the electrons is seen around the O—H bonds and around the nearest framework oxygens. This is indicative of strong hydrogen bonding stabilizing the methoxonium ion. The binding energy, relative to the isolated zeolite and vapor phase methanol, is found to be 82 kJ mol⁻¹. By repeating the calculation of the binding energy with a higher energy cutoff, we estimate the basis set error in this value to be less than 2 kJ mol⁻¹. The value for the binding energy is within the large range of experimental estimates, which range from⁴² 63 to⁹ 120 kJ mol⁻¹. However, it is not as exothermic as the extrapolation of cluster calculations to large systems would suggest, which may be indicative of artificial cluster boundary interactions. Section 5 considers the characterization of this complex in more detail.

4.2. Six-Membered Ring, Bridging across Si. One could also consider an arrangement similar to that discussed earlier, with methanol bridging between a Brønsted site and another oxygen elsewhere in the structure. We have considered the simplest possibility for this adsorption geometry that avoids a large amount of steric hindrance: that of the molecule still lying in the eight-ring window, but bridging across an Si atom adjacent to the Al. When starting with the proton on the methanol, there appears to be a very shallow local energy minimum in this case, with the acidic hydrogen midway between the methanol oxygen and the framework oxygen at a distance of 1.21 Å from each. The minimization seemed to stop here, and small displacements of the proton away from this point increased the energy. However, starting with the proton close to the framework oxygen gave the minimum energy structure illustrated in Figure 6, which has an energy about 10 kJ mol⁻¹ lower than that with the proton situated midway between the framework and methanol. The framework O—H distance is about 15% longer than that in the zeolite alone, and the distance from the proton to the methanol oxygen is very short at only 1.3 Å. In looking at the charge density, illustrated in Figure 7, very strong polarization of the methanol oxygen towards the proton is seen, which might suggest that this is more than simple hydrogen bonding and that the bond also has some covalent character. In this case, the question of proton transfer appears to be much more delicate, probably due to the fact that the other hydrogen bond, to an oxygen not adjacent to aluminum, is much weaker, with a nonbonded O—H distance of 1.96 Å. It would

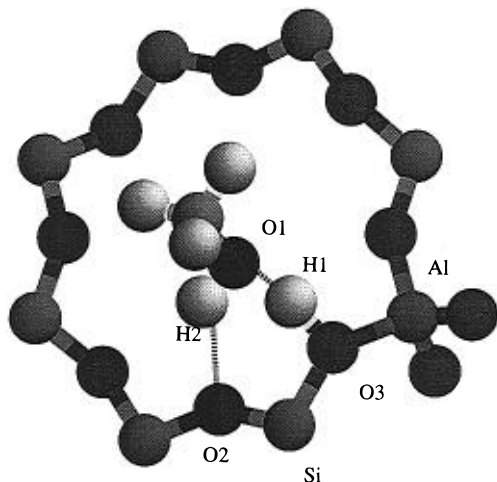


Figure 6. Equilibrium geometry found for six-membered-ring geometry, bridging across an Si site adjacent to an Al site. Distances and angles are given in Table 2.

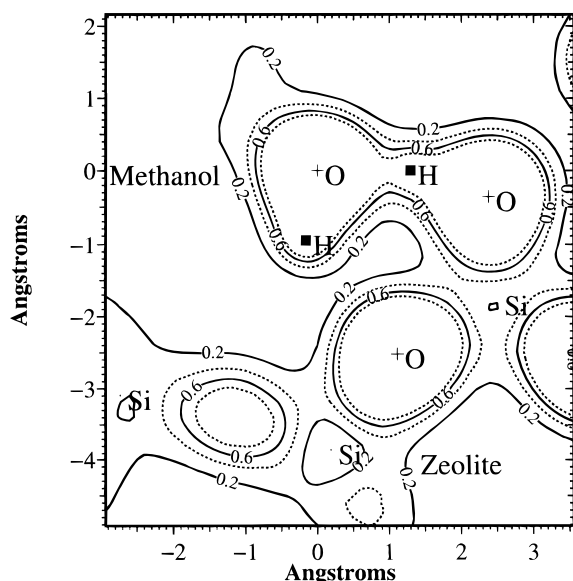


Figure 7. Valence charge density for methanol adsorbed as shown in Figure 6. Contours are in $e \text{ \AA}^{-3}$.

seem that the lack of a second very short, strong hydrogen bond causes the protonated form to be less stable. This weaker bond is also reflected in the lower binding energy of 53 kJ mol^{-1} , although the geometry nonetheless appears to be a local minimum for adsorption.

4.3. Side-on Geometry, Bridging across Al. Another possibility is that of the C–O bond lying across the Al atom, allowing the methanol OH group to interact with the zeolite proton and the methyl group to interact with another oxygen bound to aluminum. Such a geometry might be an important intermediate in the formation of methoxy groups on the zeolite framework. We have investigated this adsorption geometry and found that it appears to produce a local minimum. The same final geometry is found starting with the proton on the framework or on the methanol, that of methanol only physisorbed, as illustrated in Figure 8. As an $(\text{OH}_2)^+$ group could only form one hydrogen bond, it is not surprising that it is unstable. The methyl hydrogens do not have any strong association with the nearby framework oxygen, the shortest $\text{CH}\cdots\text{O}$ distance being 2.45 \AA . Thus, the binding energy of 32 kJ mol^{-1} is even lower than that for the geometries previously discussed, which further demonstrates the need for two strong hydrogen bonds to assist proton transfer.

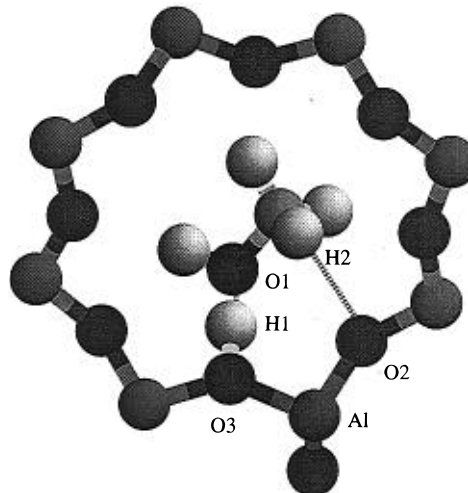


Figure 8. Equilibrium geometry found for methanol lying with the C–O bond bridging across the Al site. Distances and angles are given in Table 2.

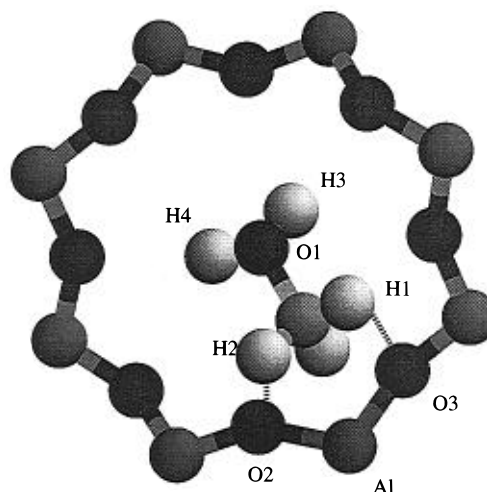


Figure 9. Equilibrium geometry found for methanol adsorbed with the methyl group coordinated to the deprotonated acid site. Distances and angles are given in Table 2.

4.4. Coordination of Methyl Group to Framework. It has been suggested from the interpretation of infrared spectra³ that in high-silica zeolites a radically different adsorption geometry of methanol may be present. In this configuration, the methoxonium is effectively rotated through 180° so that the methyl group directly coordinates to the negatively charged aluminum defect of the framework, while the $(\text{OH}_2)^+$ group resides in the center of the eight-ring window. This has been rationalized⁴³ in terms of hard and soft acid–base theory—the softer methyl group preferentially binding to the zeolite framework when the Si:Al ratio is high. Our study should correspond to this regime, and hence, in this interpretation, this adsorption geometry should represent the favored minimum.

Although our results suggest that this unusual geometry does represent an energy minimum, illustrated in Figure 9, the overall heat of adsorption is endothermic to the extent of 82 kJ mol^{-1} . We can therefore conclude that it is highly unlikely that this structure is responsible for the change in the infrared spectrum observed. The C–O bond is found to be lengthened significantly from 1.46 to 1.51 \AA , with an opening of the H–C–H angles indicating that the species can be viewed as having partial carbenium ion+water character. This is not surprising since this reversed methoxonium cation is destabilized by the increased charge separation in the ion-pair complex and by the

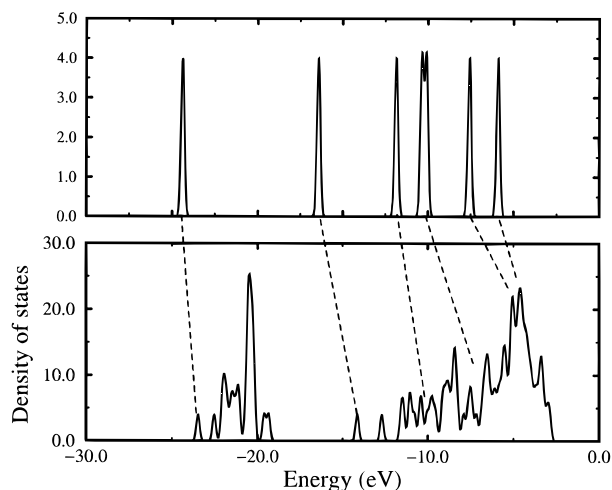


Figure 10. Electronic density of states for isolated methanol (top) and for methanol adsorbed at a Brønsted acid site in chabazite (bottom). The density of states is in eV^{-1} , smeared by a Gaussian of width 0.1 eV.

hydrophobic nature of the siliceous region of the zeolite structure.

5. Characterization of the Adsorbed Complex

The results of the previous section show that the most stable adsorption geometry is that of a methoxonium ion bridging across two oxygens adjacent to Al in the plane of the eight-ring window. Although the other geometries, in particular the sideways orientation, may be important intermediates in the subsequent reaction pathways, at a typical operating temperature of 700 K the initial adsorbed species would be expected to be of this form. We now proceed to consider the characterization of this adsorbed complex in more detail.

5.1. Charge Density and Nature of Bonding. The total charge density of the adsorbed complex is illustrated in Figure 5, showing the proton transferred from the zeolite to the methanol. We now proceed to examine this binding in terms of the individual electronic states. The electronic density of states for isolated methanol and for the adsorbed methanol/chabazite complex are illustrated in Figure 10 and can be compared to that discussed for chabazite alone. The lowest methanol orbital, consisting largely of C–O bonding, remains as a separate state upon adsorption, but examination of the charge density of this state shows that in the adsorbed protonated molecule some of the charge is transferred from C to O. Thus, adsorption on the zeolite catalyst will make the carbon atom more susceptible to nucleophilic attack. The third lowest methanol orbital, which is visibly localized on the O–H bond, becomes spread over the OH_2 group and hybridizes with the p orbitals of the two nearest framework oxygens transverse to the Si–O bonds and pointing toward the adsorbate. These transverse p orbitals thus are greatly lowered in energy compared to the others of the framework oxygens, which form a group starting some 4 eV higher in energy. The other methanol states, C–H bonds and oxygen lone pairs, are largely unchanged upon adsorption, although the highest four do have some mixing with the framework p states with which they are approximately degenerate in energy.

The description of this adsorbed form as involving charge transfer is supported by Mulliken analysis, which allocates a total charge of +0.77 to the CH_3OH_2 group.⁴⁴

5.2. The Potential Energy Surface (PES) of Proton Transfer. As remarked earlier, the result that the proton is transferred from the framework is particularly interesting, given

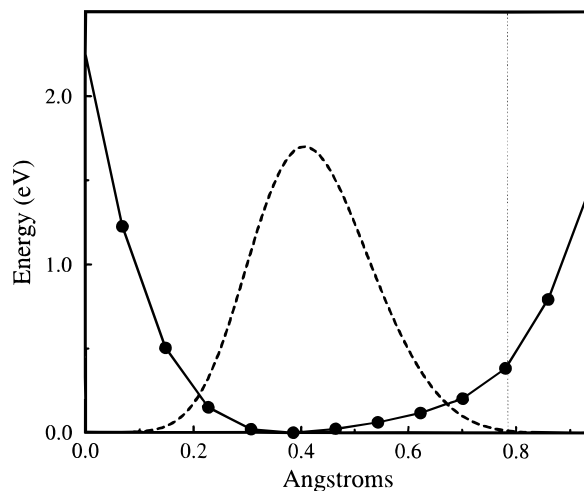


Figure 11. Calculated potential energy surface (solid line) for a proton moving between adsorbed methanol and zeolite framework and ground state probability distribution (dashed line) for a proton in such a potential. The vertical dotted line indicates where the proton would lie in the absence of the adsorbate.

that it qualitatively disagrees with previous work. We have investigated the potential energy surface of this transfer, using for simplicity the fixed-framework approximation. Although framework changes may have an important effect, our approximation is probably valid for small time scales—the proton is much lighter than the framework atoms and so will move more rapidly.

The equilibrium position of the proton in the absence of methanol was found, and the energy in the presence of methanol was then calculated for the proton at various points along the direction of the line between this position and the equilibrium position in the presence of the adsorbate. The results are plotted in Figure 11 and show that there is only one minimum, corresponding to the chemisorbed species found, but that the PES is very flat for small displacements toward the framework. This can be attributed to the strong hydrogen-bonding interaction with the framework oxygen.

In all of the calculations, the atoms themselves have been treated as classical point particles. Given the shallow potential and the light mass of the proton, it is possible that quantum mechanical effects may become important. We have treated this by using a simple model consisting of the PES shown in Figure 11 and infinite potential walls at the edges of the region shown. This is probably reasonable, as the proton will be strongly repelled by the oxygen nuclei at very close distances, and has the convenience of allowing the proton wave function to be expanded in sine functions. By using a finite number of basis functions and a fourth-order polynomial fit to the form of the PES, the ground state wave function may then be found by matrix diagonalization. The probability distribution for the ground state using 50 basis functions is also plotted in Figure 11; no visible change is seen on such a plot if twice the number of basis functions are used. This distribution has a maximum very close to the classical equilibrium position and a half-maximum half-width of about 0.13 Å. Therefore, to some extent the proton is delocalized in the region midway between the methanol and zeolite, although not as far as its position in the absence of adsorbate. This confirms that the proton is transferred from the zeolite to the methanol, but with large uncertainty in its exact position due to quantum effects.

5.3. IR Frequency Calculations. As mentioned earlier, the interpretation of IR spectra of methanol adsorbed on zeolites has been a matter of debate. O–H stretching bands in the region

TABLE 3: Calculated IR Frequencies (cm⁻¹) in the Harmonic Approximation^a

	C-H stretch	C-O stretch	O-H stretch	H-O-H bend
methanol	3045 2980 2920	1010	3890	
<i>expt.</i>	2850–3000	1020	3680	
methoxonium	3145 3135 3015	857	3760 3680	1640
methanol + chabazite	3120 3090 3000	1015	2757 2009	1583

^a The experimental values are for vapor phase methanol taken from Aldrich.⁴⁵ The adsorption geometry is the most stable six-membered-ring structure, where proton transfer to the adsorbate takes place.

of 2000–2900 cm⁻¹ have been interpreted as symmetric and antisymmetric stretching of protonated methanol molecules, but this has been difficult to reconcile with the results of cluster calculations, leading to other explanations being proposed. As analytic second derivatives are not available with the code used, we have calculated the IR frequencies of this complex in the harmonic approximation by using finite displacements of the atoms by ± 0.01 and ± 0.02 Å in each Cartesian direction. To reduce the time taken to find the ground state electronic configuration of the displaced system, the wave function of the equilibrium configuration was used as the starting point each time. Linear fitting of force against displacement was used to construct the dynamical matrix, which could then be diagonalized to find the normal modes and frequencies.

The results of calculations for isolated methanol, isolated methoxonium, and the adsorbed complex are listed in Table 3. In the first two cases the full dynamical matrix was calculated, but in the last case, to avoid a prohibitively large number of calculations, it was assumed that the motion of the OH₂ group and a few neighboring atoms could be decoupled from the rest of the framework. The O–H stretching frequencies, when only considering the OH₂ group, were calculated as 2755 and 1997 cm⁻¹; when considering the whole (CH₃OH₂)⁺ they were 2756 and 2004 cm⁻¹, and when also including the two closest framework oxygens the frequencies were 2757 and 2009 cm⁻¹. We therefore assume that the remaining coupling error in the final set, which is given in Table 3, is negligible. It is seen that for methanol the calculated frequencies fall a little above the experimental ones for O–H stretching, but an estimate of the anharmonicity correction using the same methods as section 3 reduces the calculated frequency to 3640 cm⁻¹.

The experimental results for methanol adsorbed in zeolites are less clear-cut, and indeed their interpretation has been a matter of debate.⁸ While we are not aware of any data for methanol in chabazite, Mirth *et al.*,³ from results for methanol adsorbed in H-ZSM-5, allocate bands at around 3500, 2900, 2440, and 1687 cm⁻¹ to O–H bonds and other bands around 2900–3000 cm⁻¹ to C–H stretching. Izmailova *et al.*⁴ find, for methanol in H-mordenite, C–H bands at 2700–3100 cm⁻¹ and O–H bands at 2700–3100, 2400–2600, and 1700–1750 cm⁻¹. These have been interpreted in terms of symmetric and antisymmetric stretching and H–O–H bending of the OH₂ group of protonated methanol molecules. However, other explanations have been proposed on the basis of an (A,B,C) triplet of a strongly hydrogen-bonded physisorbed complex.⁴⁶

Our calculated O–H stretching modes are actually found to correspond to separate modes for each O–H bond, an effect of the asymmetry of the nonbonded O···H distances. However, the strong hydrogen bonding makes the potential energy surface

for some atomic displacements very flat, as seen in section 5.2. A slightly different arrangement could be found for the atoms in the same sort of geometry, but with O···H distances more symmetric and an energy only 2 kJ mol⁻¹ higher (less than kT at room temperature). This gave calculated O–H stretching frequencies of 2490 and 2150 cm⁻¹, corresponding to antisymmetric and symmetric modes of the OH₂ group, respectively. Further uncertainty may be present in these frequencies due to quantum effects on the proton positions. Such variation in frequencies would explain the very broad nature of the experimentally measured peaks. From our results, we would suggest that only the broad bands in the region 2000–2700 cm⁻¹ can be attributed to O–H stretching of protonated methanol molecules, the frequencies being strongly red-shifted compared to free O–H groups due to the hydrogen-bonding effects. The bands around 2900 cm⁻¹ are attributed, from our results, to be solely due to C–H stretching, in agreement with the unpublished results quoted in ref 47. The band around 1700 cm⁻¹ is shown to be due to H–O–H bending of protonated methanol molecules. The band at 3500 cm⁻¹ seen by Mirth *et al.* is not found in our work—it may be due to Brønsted acid sites where no methanol is adsorbed or methanol is adsorbed in a different way (see section 6). In the work of Hasse and Sauer,⁹ it is concluded that the vibrational frequencies obtained from the ion–pair complex as a transition state are inconsistent with the experimentally observed spectra. However, we find in our calculations of the methoxonium ion as a stable species that the modes are far less red-shifted than their work suggests.

The comparatively low O–H stretching frequencies in the adsorbed complex are another indication of the strength of hydrogen bonding involved in the adsorption process. This is consistent with the large proton deshielding effects noticed in *in situ* NMR experiments.⁵ It is notable that, despite the increased polarization of the C–O bond observed earlier, the stretching frequency is not reduced by as much as it is in free methoxonium, probably again due to hydrogen bonding stabilizing the OH₂ group. The methyl group seems to be largely unaffected by protonation or by adsorption.

5.4. Framework Distortions. The local geometry of the zeolite around the adsorbate is shown in Figure 4. Since our work includes the full zeolite structure with the optimization of all atomic positions, we can also examine distortions of the rest of the framework. If the framework in the absence of methanol is distorted from the stable geometry to the configuration that it adopts for adsorption (but allowing the proton to remain on the framework), we find that this increases the energy by 32 kJ mol⁻¹, which is small in comparison with the energy of 145 kJ mol⁻¹ required to then increase the proton framework distance from the equilibrium 0.98 to 1.4 Å. However, substantial changes on the order of 5–10° are seen in the Al–O–Si angles around the active site and also in the nearest neighbor Si–O–Si angles. These are presumably important in allowing the formation of the short, strong hydrogen bonds observed in our calculations. Although the O–Al–O angle changes noticeably, other O–Si–O angles change very little, consistent with the observation that the force constant for bending of the O–Si–O angles is much greater than for Si–O–Si angles.⁴⁸ There is no sign of large displacements of oxygens on the far side of the eight-ring toward the methyl hydrogens, although this could be due to the unit cell size. The eight-ring diameter is about 7 Å and the unit cell length is 9 Å, so that on the far side distortions could be dominated by effects from the next periodic image of the complex.

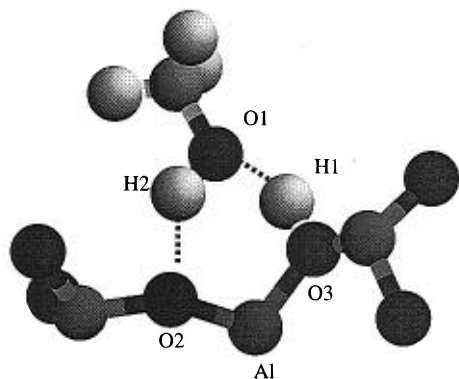


Figure 12. Calculated equilibrium geometry for methanol adsorbed in sodalite, bridging across two oxygens on either side of Al.

6. Effect of Structure on Reactivity

We have shown that our periodic calculations using the full zeolite structure of chabazite give results that are qualitatively different from cluster-based calculations. Other work using first-principles molecular dynamics to study methanol adsorption in a periodic zeolite model⁴⁷ has shown methanol to be only physisorbed. These authors also used gradient-corrected density functional methods, although implemented in a slightly different way. However, the major difference is their choice of a high-silica form of the sodalite structure.⁴⁹ Therefore, to examine the possible effect of framework topology on the nature of adsorption, we have repeated some of our calculations using such a structure.⁵⁰ Like chabazite, sodalite has 36 atoms in the unit cell. However, the structure is quite different: chabazite has eight-ring channels, whereas sodalite consists of large open cages linked by six-ring and four-ring windows. Although sodalite itself is an artificial case, as it does not have pores into which methanol can penetrate, the sodalite cage is an important subunit in several more complex zeolite structures such as zeolite-A.

6.1. Adsorption Geometry. Initially we consider the analogue of the most stable adsorption geometry found in chabazite. The smaller rings of sodalite mean that the methyl group must point into the sodalite cage rather than being able to lie in the channel. In this case, when starting with the proton on the framework or on the methanol, the same final equilibrium geometry is found, that of methanol being simply physisorbed. The hydrogen bonding of this complex would not appear to be as strong as that of the chemisorbed form, as seen by the longer nonbonded O...H distances illustrated in Figure 12. It is seen that the framework proton makes a strong hydrogen bond with the methanol, of distance 1.58 Å, but the hydrogen bonding between the methanol proton and the framework is weaker, with an O...H distance of 1.90 Å. The small ring size in sodalite means that another geometry is possible, where the methanol proton is coordinated with an oxygen on the far side of the six ring.⁴⁷ We investigated this and found the equilibrium geometry illustrated in Figure 13. In this case, the interaction of the methanol proton with the framework oxygen actually appears stronger, with the distance falling to 1.76 Å. However, again no proton transfer is observed. Thus, our results confirm those found by Nusterer *et al.*⁴⁷

Interestingly, the binding energy for this physisorption, at 68 and 73 kJ mol⁻¹, respectively, for the two geometries, is not much smaller than that found for chemisorption in chabazite. This suggests that there is an energy penalty for proton transfer that is offset by strong hydrogen bonding for the methoxonium ion. Depending on the framework effects, either the chemisorbed or the physisorbed state is the stable form. From these

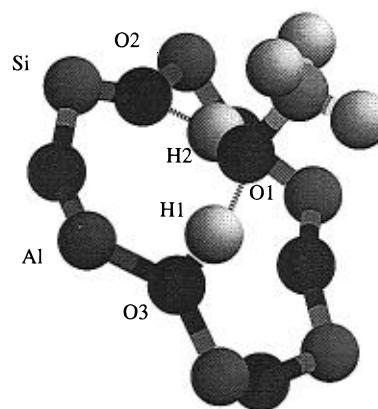


Figure 13. Calculated equilibrium geometry for methanol adsorbed in sodalite, bridging across to the far side of the six ring.

results it would appear that if methanol is in an open cage physisorption is favored, but when the methanol can lie in a ring the charge transfer due to chemisorption is stabilized by the electrostatic potential and/or interactions with the far side of the ring. Given that chabazite is the structure that exhibits catalytic activity for methanol adsorption, it is likely to be the more realistic model of the real catalyst. We would therefore speculate that it is the chemisorbed form of methanol that is required for the subsequent reaction to take place. The commercial catalyst, ZSM-5, has rings large enough for methanol to lie in, so that our results suggest that methanol may be chemisorbed at some of the Brønsted acid sites in ZSM-5.

6.2. Infrared Spectrum. We have calculated the IR spectrum for methanol adsorbed in sodalite by using the same method that was used for chabazite. In this case we focus only on the motion of the O-H groups, since the previous results suggested that coupling of the motion of these groups to the rest of the material was negligible. In this case, the O-H stretching frequencies have two distinct modes: one at 3565 cm⁻¹ (methanol OH) and one at 2160 cm⁻¹ (framework OH). O-H bending modes are seen at 1420 and 1050 cm⁻¹. These can be compared to the frequencies found for the chemisorbed form in chabazite. Both forms give O-H stretching frequencies in the 2000–3000 cm⁻¹ range caused by strong hydrogen bonding. Physisorbed methanol also gives a characteristic band at 3500 cm⁻¹. Chemisorbed methanol can be distinguished by the higher frequency of the H-O-H bending mode at about 1700 cm⁻¹, which can be attributed to a methoxonium ion.

7. Conclusions

The results presented in this work represent the first detailed energy minimization study of methanol adsorption in zeolites using periodic boundary conditions, as opposed to the more conventional use of cluster models. The consideration of specific zeolite materials rather than generic fragments is found to be essential for a complete understanding of the adsorption process, as we find that there is a strong correlation between the local framework structure and the adsorbed state of methanol. In particular, on the basis of the behavior observed in the cases of sodalite and chabazite, we predict that methanol will be physisorbed only in open cage regions of the structure, whereas the presence of eight, and quite probably ten, rings leads to the protonation of methanol without a barrier.

There has been recent speculation based on cluster calculations¹⁰ that the formation of surface-bound methoxy groups, thought to be an important intermediate in the reactions of methanol within zeolites, is not dependent on the protonation of methanol. However, it is probable that the activation energy

would be reduced when starting from the ion-pair complex rather than from the neutral pair, as the framework O—H bond is already broken. Hence, it is likely that the medium-aperture windows represent the most active sites for catalysis, when taking into account both the protonation of methanol and the proximity of suitable oxygens for methylation. Further work, using the present methodology, is currently in progress to characterize possible reaction pathways for methanol in an aluminosilicate environment.

Examination of the binding of methanol in both chabazite and sodalite demonstrates that a variety of possible energy minima exist, not all of which involve the adsorbate forming a hydrogen-bonded complex bridging across the aluminum defect site. Provided that a second hydrogen bond can be formed by the methanol hydrogen to supplement that formed by the framework proton, an adsorption energy close to that of the conventional geometry will result. In the case of chabazite, a possible alternative geometry is for methanol to straddle a silicon atom within the eight-ring window, while in sodalite the molecule may bridge across the six ring.

Calculations of infrared frequencies give a prediction for the spectrum of methanol adsorbed in chabazite and show differences with the spectrum of the physisorbed form found in the sodalite case. Given the variety of available adsorption sites, it is difficult to use these results to make a definitive interpretation of the experimental infrared spectra. Most experimental studies are on the material H-ZSM-5, and until it is feasible to directly study this system, we cannot exclude the possibility that only the physisorbed species is present and that the observed spectrum results from resonance between bands. However, the set of frequencies obtained by combining the results calculated for both the chemisorbed and physisorbed complexes is likely to be sufficient to explain the main vibrational characteristics seen experimentally, if it is assumed that the species are present in equilibrium with one another.

In conclusion, we have shown that the use of periodic density functional theory is an efficient and reliable method for obtaining detailed information on molecular adsorption in microporous materials. Further work in progress should allow us to gain a more detailed insight into the correlation between zeolite structure and catalytic activity.

Acknowledgment. These calculations were performed on the Cray T3D in Edinburgh as part of the UKCP and the Materials Chemistry consortium. J.D.G. thanks the Royal Society and R.S. thanks EPSRC for financial support. We are grateful to M. H. Lee for assistance with pseudopotentials.

Appendix: Estimation of Anharmonic Effects Using the Morse Potential Model

Use of a quadratic fit to energy against displacement for small changes in bond length allows the straightforward estimation of vibrational frequencies in the harmonic approximation. However, for estimates of anharmonicity, modeling of the potential by a higher order polynomial is, in general, unsatisfactory as this has incorrect long-range behavior. A suitable model with the correct long-range behavior is the well-known Morse potential:

$$E = A(1 - \exp(-\alpha(x - x_0)))^2 + B \quad (1)$$

which for small displacements from the equilibrium distance x_0 can be approximated to the third order as

$$E = B + A\alpha^2(x - x_0)^2 - A\alpha^3(x - x_0)^3 \quad (2)$$

Thus, from a third-order polynomial fit for small displacements the parameters A , B , α , and x_0 of the Morse potential can be extracted. The harmonic frequency ω_0 is obtained by

$$A\alpha^2 = \frac{1}{2}\mu\omega_0^2 \quad (3)$$

where μ is the reduced mass of the two atoms.

However, in a Morse potential the energy levels are given by

$$E_n = \left(n + \frac{1}{2}\right)\hbar\omega_0 - \left(n + \frac{1}{2}\right)^2 \frac{\alpha^2\hbar^2}{2\mu} \quad (4)$$

As the experimental frequency will be $(E_1 - E_0)/\hbar$, this gives the anharmonicity-corrected frequency as

$$\omega' = \omega_0 \left(1 - 2\frac{\alpha^2\hbar}{2\mu\omega_0}\right) \quad (5)$$

References and Notes

- (1) Thomas, J. M. *Philos. Trans. R. Soc. London A* **1990**, 333, 173.
- (2) Meisel, S. L.; McCulloch, J. P.; Lechthaler, C. H.; Weisz, P. B. *Chem. Tech.* **1976**, 6, 86.
- (3) Mirth, G.; Lercher, J. A.; Anderson, M. W.; Klinowski, J. *J. Chem. Soc., Faraday Trans.* **1990**, 86, 3039.
- (4) Izmailova, S. G.; Karetina, I. V.; Khvoshchev, S.; Shubaeva, M. A. *J. Colloid Interface Sci.* **1994**, 165, 318.
- (5) Anderson, M. W.; Klinowski, J. *Nature* **1989**, 339, 200.
- (6) Klinowski, J. *Anal. Chim. Acta* **1993**, 283, 929.
- (7) Sauer, J.; Kölmel, C.; Haase, F.; Aldrichs, R. In *Proceedings of the 9th International Conference on Zeolites*; von Ballamos, R., Higgins, J. B., Treacy, M., Eds.; Butterworths: London, 1993; p 679.
- (8) Gale, J. D.; Catlow, C. R. A.; Carruthers, J. R. *Chem. Phys. Lett.* **1993**, 216, 155.
- (9) Haase, F.; Sauer, J. *J. Am. Chem. Soc.* **1995**, 117, 3780.
- (10) Zicovich-Wilson, C. M.; Viruela, P.; Corma, A. *J. Phys. Chem.* **1995**, 99, 13224.
- (11) Blaszkowski, S. R.; van Santen, R. *J. Phys. Chem.* **1995**, 99, 11728.
- (12) Kramer, G. J.; van Santen, R. A.; Emeis, C. A.; Nowak, A. K. *Nature* **1993**, 363, 529.
- (13) Allavena, M.; Kassab, E. *Solid State Ionics* **1993**, 61, 33.
- (14) Greatbanks, S. P.; Sherwood, P.; Hillier, I. H. *J. Phys. Chem.* **1994**, 98, 8134.
- (15) Pisani, C.; Cora, F.; Nada, R.; Orlando, R. *Comput. Phys. Commun.* **1994**, 82, 139.
- (16) Teunissen, E. H.; Roetti, C.; Pisani, C.; de Man, A. J. M.; Jansen, A. P. J.; Orlando, R.; van Santen, R. A.; Dovesi, R. *Modelling Simul. Mater. Sci. Eng.* **1994**, 2, 921.
- (17) Campana, L.; Selloni, A.; Weber, J.; Pasquarello, A.; Papai, I.; Goursoot, A. *Chem. Phys. Lett.* **1994**, 226, 245.
- (18) Dent, L. S.; Smith, J. V. *Nature* **1958**, 181, 1794.
- (19) Tintskaladze, G. P.; Nefedova, A. R.; Gryaznova, Z. V.; Tsitsishvili, G. V.; Charkviani, M. K. *Zh. Fiz. Khim.* **1984**, 58, 718.
- (20) Payne, M. C.; Teter, M. P.; Allan, D. C.; Arias, T. A.; Joannopoulos, J. D. *Rev. Mod. Phys.* **1992**, 64, 1045.
- (21) Hohenberg, P.; Kohn, W. *Phys. Rev.* **1964**, 136, B864.
- (22) Kohn, W.; Sham, L. J. *Phys. Rev.* **1965**, 140, A1133.
- (23) Perdew, J. P. In *Electronic Structure of Solids '91*; Zeisler, P., Eschrig, H., Eds.; Akademie Verlag: Berlin, 1991.
- (24) White, J. A.; Bird, D. A. *Phys. Rev. B* **1994**, 50, 4954.
- (25) Bachelet, G. B.; Hamman, D. R.; Schluter, M. *Phys. Rev. B* **1982**, 26, 4199.
- (26) Lee, M.-H.; Lin, J. S.; Payne, M. C.; Heine, V.; Milman, V.; Crampin, S. *Phys. Rev. B* **1995**, submitted.
- (27) Lin, J. S.; Qteish, A.; Payne, M. C.; Heine, V. *Phys. Rev. B* **1993**, 47, 4174.
- (28) King-Smith, R. D.; Payne, M. C.; Lin, J. S. *Phys. Rev. B* **1991**, 44, 13063.
- (29) Lee, M.-H. *Improved optimised pseudopotentials and application to disorder in γ -Al₂O₃*. Ph.D. Thesis, University of Cambridge, Cambridge, UK, 1995.
- (30) Shah, R.; De Vita, A.; Payne, M. C. *J. Phys.: Condensed Matter* **1995**, 7, 6981.
- (31) Leslie, M.; Gillan, M. J. *J. Phys. C* **1985**, 18, 973.

- (32) Makov, G.; Payne, M. C. *Phys. Rev. B* **1995**, *51*, 4014.
- (33) Aue, D. H.; Bowers, M. T. In *Gas phase ion chemistry*; Bowers, M. T., Ed.; Academic Press: New York, 1979; Vol. 2.
- (34) Press, W. H.; Flannery, B. P.; Teukolsky, S. A.; Vetterling, W. T. In *Numerical Recipes in Fortran*; Cambridge University Press: New York, 1992; Chapter 10, pp 418–420.
- (35) Clarke, L. J.; Stich, I.; Payne, M. C. *Comput. Phys. Commun.* **1992**, *72*, 14.
- (36) Shah, R.; Gale, J. D.; Payne, M. C. *Int. J. Quant. Chem.* **1996**, in press.
- (37) Cheetham, A. K. Personal communication.
- (38) Mix, H.; Sauer, J.; Schroder, K. P.; Merkel, A. *Collect. Czech. Chem. Commun.* **1988**, *53*, 2191.
- (39) Sauer, J. In *Modelling of structure and reactivity in zeolites*; Catlow, C. R. A., Ed.; Academic Press: London, 1992; p 183.
- (40) Apra, E.; Dovesi, R.; Freyria-Fava, C.; Pisani, C.; Roetti, C.; Saunders, V. R. *Modelling Simul. Mater. Sci. Eng.* **1993**, *1*, 297.
- (41) Carpenter, J.; Gale, J. D.; Catlow, C. R. A. Manuscript in preparation.
- (42) Messow, U.; Quitzsch, K.; Herden, H. *Zeolites* **1984**, *4*, 255.
- (43) Mirth, G.; Kogelbauer, A.; Lercher, J. A. In *Proceedings of the 9th International Conference on Zeolites*; von Ballamos, R., Higgins, J. B., Treacy, M., Eds.; Butterworths: London, 1993; p 251.
- (44) Segall, M. D.; Pickard, C. J.; Shah, R.; Payne, M. C. *Mol. Phys.* **1996**, in press.
- (45) Pouchert, C. J. *The Aldrich Library of FT-IR Spectra*, 1st ed.; Aldrich Chemical Company: Milwaukee, WI, 1989.
- (46) Pelenschikov, A.; van Wolput, J.; Janchen, J.; van Santen, R. *J. Phys. Chem.* **1995**, *99*, 3612.
- (47) Nusterer, E.; Blöchl, P. E.; Schwarz, K. *Angew. Chem.* **1996**, *35*, 175.
- (48) Putnis, A. In *Introduction to Mineral Sciences*; Cambridge University Press: Cambridge, U.K. 1992; Chapter 6, p 141.
- (49) Bibby, D. M.; Dale, M. P. *Nature* **1985**, *317*, 157.
- (50) Shah, R.; Gale, J. D.; Payne, M. C.; Lee, M.-H. *Science* **1996**, *271*, 1395.

JP960365Z